JOURNAL OF MAGNETIC RESONANCE **129,** 1–9 (1997)
ARTICLE NO. MN971224

# Internal Rotation of Mutually Interacting Methyl Groups: A $^{13}C$ NMR Study

Reinhard Wimmer[1] and Norbert Müller[2]

*SINTEF UNIMED MR-Center, N-7034 Trondheim, Norway; and Institute of Chemistry, Johannes-Kepler-University, Altenbergerstrasse 69, A-4040 Linz, Austria*

Received April 1, 1997; revised July 10, 1997

**The overall and intramolecular rotational diffusion behavior of 1,3,7,10-tetramethylbenzo[*c*]cinnoline was determined from longitudinal $^{13}C$ NMR relaxation and {$^1H$}–$^{13}C$ NOE measurements in dilute chloroform solution. The four methyl groups in this compound represent three different situations of sterical hindrance. One pair of methyl groups is in close mutual sterical contact, forming the ends of an open six-membered ring. Assuming completely anisotropic overall molecular tumbling combined with a 120° jump model for the internal methyl rotations the jump rates of methyl groups were evaluated and compared to earlier results on different sterically hindered compounds, in particular with respect to a potential cogwheel-like intermethyl interaction. To characterize intermethyl interactions in different sterical situations, a new gauge—the "methyl interaction volume"—is introduced. Implications for correlated rotational diffusion of methyl groups are discussed.** 

## INTRODUCTION

Internal rotations of methyl groups are the fastest intramolecular rotations in organic molecules. The slowdown of this motion through sterical hindrance is of high theoretical interest in the context of motional correlation and still unresolved questions of methyl tunneling. To our knowledge compounds of the 4,5-dimethylphenanthrene type (**I** in Fig. 1), which have previously been the subject of studies with respect to the skeletal deformation caused by the steric interaction of the substituents (*1, 2*) and the effect of ring distortion on the electrophilic aromatic reactivity (*3*), have never been used before to assess the influence of the sterical hindrance on the internal rotation of the methyl groups.

The primary goal of this work was to compare the internal rotational diffusion constants of both ''unhindered'' methyl groups and mutually strongly sterically hindered methyl groups attached to the same rigid molecular frame in solution state. A juxtaposition of methyl groups in an open six-membered ring bears the potential of a cogwheel interaction. The effect of such an interaction on the internal jump rates is of special interest in view of the possibility of correlated methyl rotation. To our knowledge comparison of the internal rotational diffusion constants of sterically free and cogwheel-like interacting methyl groups in a single molecule has not been attempted previously.

Among the compounds suitable for such an investigation 1,3,7,10-tetramethylbenzo[*c*]cinnoline (**II**) was chosen mainly for reasons of availability, solubility, and stability. Its synthesis will be described elsewhere.

The evaluation of $^{13}C$ dipolar longitudinal relaxation data is the most common approach to overall and intramolecular motions [see, e.g., (*4–9*)]. In the following section we briefly summarize the theory relevant in this particular context.

## THEORY

$^{13}C$ relaxation in solution is predominantly caused by intramolecular dipolar interactions with protons. In the limit of extreme narrowing, the longitudinal relaxation time through the dipolar pathway, $T_{1dd}$, can be determined from the overall longitudinal relaxation time $T_1$ and the heteronuclear Overhauser effect $\eta$ (*10*):

$$\frac{1}{T_{1dd}} = \frac{1}{T_1} * \frac{\eta}{\eta_{max}} . \qquad [1]$$

As will be shown below, all experiments were run under extreme narrowing conditions, so that Eq. [1] holds.

The effects of overall and internal rotations on dipolar relaxation times have been derived analytically by Woessner (*11–13*). His approach uses a number of approximations based on symmetry properties of the overall motion and the relative orientation of the axis of internal rotation to symmetry axes of the overall molecular rotation. The most general case, totally anisotropic overall molecular motion together

[1] Present address: Institut f. Molekularbiologie und Biophysik, ETH-Hönggerberg, CH-8093 Zürich, Switzerland.
[2] To whom correspondence should be addressed at the Johannes-Kepler-University. E-mail: Norbert.Mueller@jk.uni-linz.ac.at.



1090-7807/97 $25.00

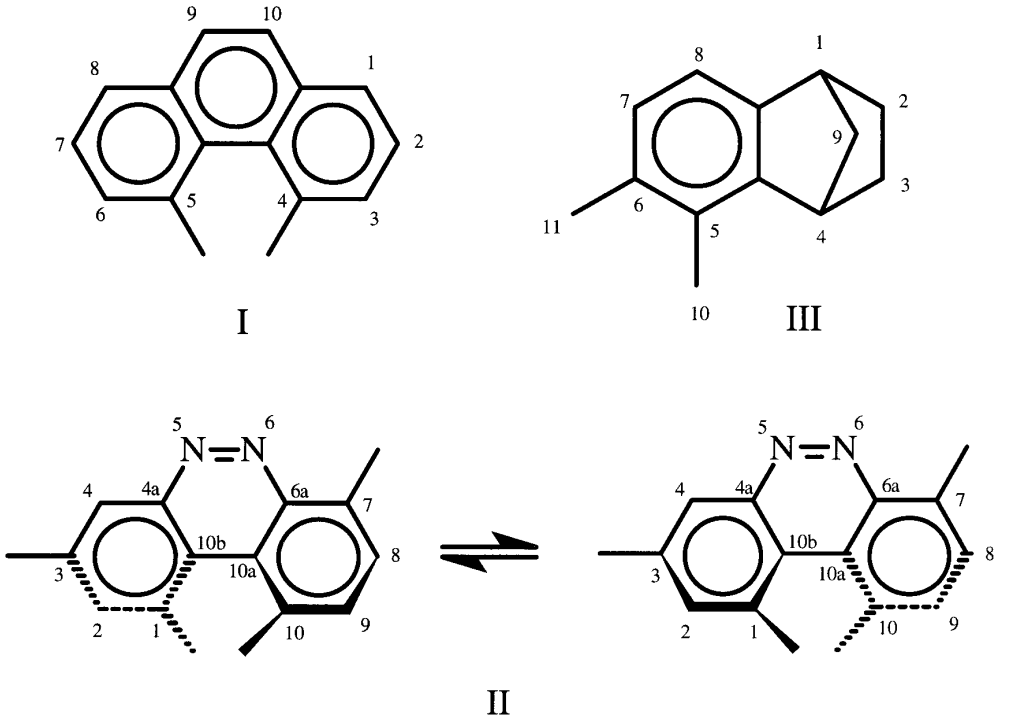


**FIG. 1.** 4,5-Dimethylphenanthrene (**I**), 1,3,7,10-tetramethylbenzo[*c*]cinnoline with its two helical enantiomers (**II**), and 1,2,3,4-tetrahydro-5,6-dimethyl-1,4-methanonaphthalin (**III**).

with any number of internal methyl group rotations at arbitrary positions in the molecule, has been treated by Bluhm (*14*). From this work the relaxation rate of a spin *I* relaxing through dipolar interaction with a single spin *S* is given by

$$\frac{1}{T_{1\mathrm{dd}}^{I}} = \gamma_I^2\gamma_S^2\left(\frac{h}{2\pi}\right)^2 S(S+1)\left[\frac{1}{12}\,J_0(\omega_I-\omega_S) + \frac{3}{2}\,J_1(\omega_I) + \frac{3}{4}\,J_2(\omega_I+\omega_S)\right]. \quad [2]$$

The dependence of the spectral density functions $J_n(\omega)$ for the reorientation of the *IS* vector on the rotational correlation times was derived in Ref. (*14*) and is reproduced in the Appendix to this paper (Eqs. [A1]–[A6]).

The inverse problem of calculating the overall and intramolecular rotational diffusion constants from the dipolar relaxation rates cannot be solved analytically. Therefore numerical methods must be applied. For this purpose we developed a computer program (using Think Pascal 4.0 (*15*) under MacOS 7.5.2). The formulas derived by Woessner (*11*) used to calculate the dipolar $^{13}$C relaxation caused by $^{1}$H nuclei attached to the rigid structure with anisotropic overall molecular motion are given in the Appendix (Eqs. [A7]–[A9]).

The effect of the $^{1}$H nuclei attached to internally rotating fragments on the $^{13}$C dipolar relaxation times is calculated by Bluhm's equations (*14*) given in the Appendix (Eq. [A1]).

The program starts from a random or arbitrarily chosen set of rotational diffusion constants and calculates the $^{13}$C dipolar relaxation times. The sum of squares of deviations of the calculated from experimentally derived $T_{1\mathrm{dd}}$ values is minimized using a steepest-descent approach while varying the overall and internal rotational diffusion constants. For the model compound **II** eight $T_{1\mathrm{dd}}$ values were used to determine three overall and four internal rotational diffusion constants. The $T_{1\mathrm{dd}}$ values of the nonprotonated carbon atoms were not used in these calculations because of their high uncertainty (Table 1), as in a similar study (*9*).

Chemical exchange between the two enantiomers of opposite helicity (see Fig. 1) is too slow at the measurement temperature to contribute to the relaxation rates. This is corroborated by the inversion barrier of a similar compound, 4,5-dimethylphenanthrene (**I**), which was determined to be 67.3 kJ mol$^{-1}$ (*1*), corresponding to an inversion rate of 0.4 s$^{-1}$ at 260.5 K.

Due to the limited number of $^{13}$C–$^{1}$H vectors and the intrinsic properties of the model compound, a number of simplifying assumptions had to be made which will be discussed in the following:

—The rotational diffusion axis system was assumed to coincide with the inertial axis system, although this is not necessar-

ily so [see (*16*) and references cited therein]. But at the actual error level of the experimental data (Table 1) a differentiation between the two axis systems as performed in Ref. (*9*) is not possible. These deviations mostly influence the calculated overall rotational tumbling rate of the molecule. Internal rotational diffusion constants calculated from these data do not depend significantly on small changes in the orientation of the axis system (*9*), as will be shown below.

—Bluhm's approach (*14*) allows for methyl group jumps between three different sites, two of which are equivalent. The most general model introduces three different jump rates per methyl group instead of one. Determining this large number of parameters requires more independent and highly accurate experimental $T_{1dd}$ values [at a 1% error level according to Ref. (*16*)]. The model compound used does not have a sufficient number of CH vectors which in addition are nearly coplanar. Therefore a model with three equivalent jumping positions was assumed by setting all three jump rates for each methyl group equal as in the study of (*9*).

—For proton-decoupled methyl carbons the effect of cross-correlation of proton–proton dipolar interactions on the NOE is neglected. This is justified when the jump rate of the internal rotation is not more than 20 times higher than the overall rotational diffusion constants (*17–22*). As will be seen below, this condition is not met for the freely rotating methyl groups 3 and 7, which most probably leads to an underestimation of their rotational diffusion constants.

We have also run preliminary $^{1}$H multiple-quantum-filtered experiments (*23, 24*) which did not show any indication of cross-correlation effects—most probably because in this motional regime the effects are expected to be very small as can be seen from the results in Ref. (*25*).

—Bluhm's treatment (*14*) is only valid if diffusion effects dominate over inertial effects for the overall molecular tumbling as well as for the internal rotations. This assumption is also problematic for the most freely rotating methyl group 3. This error has, however, little influence on the sterically hindered methyl groups, which are of prime interest in this study.

—Another restriction, which is inherent to Bluhm's approach (*14*), is that completely independent molecular motions are assumed. So far the experimental data show no evidence for correlated methyl rotation. Should such a correlation be discovered later, the model might need to be adjusted accordingly.

—Due to the low signal-to-noise ratio at the concentration used it was not possible to access additional experimental information such as $^{13}$C multiplet asymmetry. This would allow one to include the CSA relaxation pathway [as done in Ref. (*26*)] and provide additional parameters, thus increasing the accuracy of the model.

## EXPERIMENTAL

All experiments were carried out on a Bruker Avance DRX-600 spectrometer equipped with a 5-mm inverse ($^{1}$H, $^{13}$C, $^{15}$N, $^{31}$P) quadrupole resonance probe with $x$, $y$, $z$ gradients and a $Q$ switch (which was however not used in these studies). All measurements were performed at 260.5 ± 0.5 K.

Seven milligrams of **II** was dissolved in approximately 0.8 ml of $CDCl_3$ (Uetikon, ⩾99.95% $^{2}$H), and oxygen was removed by several (approximately 10) freeze–pump–thaw cycles, until the amount of solvent was decreased to approximately 0.5 ml, giving a final concentration of ~0.06 mol liter$^{-1}$. The sample was sealed *in vacuo*. The low concentration was used to avoid intermolecular stacking interactions. The temperature of 260.5 K was chosen in order to slow down the overall tumbling to within the diffusion range (but still in the extreme narrowing) so that it is not dominated by inertial effects (*10*).

$^{13}$C longitudinal relaxation times were measured by the inversion-recovery method, using an inversion pulse of 24.4 $\mu$s and a decoupling field (WALTZ) of 2.5 kHz centered at 4.5 ppm with power gating to 1.25 kHz during a recycle delay of 24 s. The relaxation times were obtained by fitting the peak height to a monoexponential decay using the computer program MacCurveFit (*27*). NOE values $\eta$ were determined from differences of decoupled $^{13}$C spectra with and without $^{1}$H irradiation during the recycle delay of 45 s (with an acquisition time of 1.8 s). The experiments were repeated five times with different delay lists after reshimming and retuning and averaged to decrease the experimental error. The inverse-gated decoupling experiments used 1024 transients, and the inversion-recovery experiments 512 transients per variable delay. Twenty-five different delays ranging from 1 ms to the length of the recycle delay were used. All data points obtained were fitted simultaneously.

Complete assignment was achieved via inverse gradient-enhanced HC correlation spectra [one-bond correlation via double INEPT transfer using sensitivity improvement, Bruker pulse program ''invieagssi'' (*28–30*), all Bruker software from the xwinnmr 1.1.1 release], long-range 2D HC correlation via heteronuclear zero- and double-quantum coherence, with low-pass $J$ filter to suppress one-bond correlations, without decoupling during acquisition, using gradient pulses for selection (Bruker pulse program ''inv4gplplrnd'') and long-range HH-COSY spectra (Bruker pulse program ''cosydclr'').

Table 1 summarizes the assignments, the $T_1$ relaxation times, the NOEs $\eta$, and the dipolar relaxation times $T_{1dd}$ for all carbon atoms of compound **II**.

The molecular geometry used in the calculations was optimized using the cff91 force field if Insight II (*31*). Figure 2 depicts the optimized structure of the molecule together with its inertial axis system as calculated by Insight II. These coordinates (given in Table 2 for reference purposes) and the experimental relaxation data in Table 1 constitute the input to the minimization program.

**TABLE 1**

**$^{13}$C Chemical Shift $\delta$, Longitudinal Relaxation Time $T_1$, NOE $\eta$, and Dipolar Relaxation Time $T_{1dd}$ at 150 MHz $^{13}$C Resonance Frequency and 260.5 ± 0.5 K for Each Carbon Atom of II[a]**

| C atom | $\delta$ (ppm) | $T_1$ (s) | $\eta$ | $T_{1dd}$ (s) | $\Delta T_{1dd}$ (s) | $\Delta$% |
|---|---|---|---|---|---|---|
| 4a | 146.6 | 5.10 | 0.17 | 61 | ±16 | 26% |
| 6a | 144.7 | 5.46 | 0.06 | 188 | ±125 | 66% |
| 3 | 137.9 | 3.88 | 0.26 | 30 | ±5 | 16% |
| 7 | 135.6 | 5.17 | 0.32 | 32 | ±5 | 15% |
| 2 | 134.7 | 1.15 | 1.68 | 1.35 | ±0.08 | 6.0% |
| 1 | 133.8 | 5.35 | 0.40 | 27 | ±3 | 12% |
| 9 | 132.8 | 1.21 | 1.63 | 1.48 | ±0.08 | 5.7% |
| 10 | 131.2 | 5.28 | 0.43 | 24 | ±3 | 12% |
| 8 | 128.6 | 0.96 | 1.64 | 1.2 | ±0.2 | 13% |
| 4 | 126.1 | 1.33 | 1.74 | 1.5 | ±0.1 | 6.6% |
| 10a | 120.8 | 4.67 | 0.07 | 129 | ±72 | 56% |
| 10b | 118.8 | 4.72 | 0.08 | 115 | ±55 | 48% |
| 1-$CH_3$ | 22.0 | 1.96 | 1.94 | 2.0 | ±0.1 | 5.1% |
| 10-$CH_3$ | 21.9 | 1.89 | 1.99 | 1.9 | ±0.1 | 5.0% |
| 3-$CH_3$ | 21.0 | 4.12 | 1.56 | 5.3 | ±0.3 | 6.3% |
| 7-$CH_3$ | 17.6 | 4.07 | 1.80 | 4.5 | ±0.3 | 5.6% |

[a] This table comprises the averages of five NOE measurements and the results from three inversion-recovery series at 150 MHz and 260.5 ± 0.5 K.

**TABLE 2**

**Cartesian Coordinates of Optimized Structure of II with Respect to Its Inertial Axis System**

| Atom | $x$ (Å) | $y$ (Å) | $z$ (Å) |
|---|---|---|---|
| N-6 | 1.007 | 2.016 | −0.006 |
| C-4a | −1.069 | 1.107 | 0.114 |
| C-6a | 1.537 | 0.772 | −0.023 |
| C-3 | −3.346 | 0.482 | 0.111 |
| C-7 | 2.912 | 0.788 | −0.171 |
| C-2 | −2.921 | −0.784 | −0.273 |
| C-1 | −1.595 | −1.133 | −0.433 |
| C-9 | 2.819 | −1.581 | 0.220 |
| C-10 | 1.445 | −1.570 | 0.379 |
| C-8 | 3.537 | −0.437 | −0.088 |
| C-4 | −2.380 | 1.452 | 0.258 |
| C-10a | 0.756 | −0.370 | 0.094 |
| C-10b | −0.607 | −0.189 | −0.080 |
| C (1-$CH_3$) | −1.384 | −2.513 | −1.017 |
| C (10-$CH_3$) | 0.863 | −2.874 | 0.878 |
| C (3-$CH_3$) | −4.815 | 0.792 | 0.275 |
| C (7-$CH_3$) | 3.705 | 2.056 | −0.390 |
| N-5 | −0.246 | 2.176 | 0.185 |
| H (10-$CH_3$) | −0.124 | −2.745 | 1.343 |
| H (10-$CH_3$) | 0.794 | −3.633 | 0.083 |
| H (10-$CH_3$) | 1.504 | −3.302 | 1.667 |
| H-8 | 4.618 | −0.498 | −0.204 |
| H-9 | 3.367 | −2.512 | 0.360 |
| H (7-$CH_3$) | 4.770 | 1.851 | −0.569 |
| H (7-$CH_3$) | 3.332 | 2.617 | −1.262 |
| H (7-$CH_3$) | 3.641 | 2.722 | 0.486 |
| H-2 | −3.691 | −1.528 | −0.472 |
| H (1-$CH_3$) | −0.396 | −2.628 | −1.482 |
| H (1-$CH_3$) | −1.529 | −3.310 | −0.270 |
| H (1-$CH_3$) | −2.111 | −2.703 | −1.825 |
| H (3-$CH_3$) | −4.977 | 1.708 | 0.860 |
| H (3-$CH_3$) | −5.302 | 0.934 | −0.705 |
| H (3-$CH_3$) | −5.344 | −0.021 | 0.796 |
| H-4 | −2.649 | 2.485 | 0.462 |

## RESULTS AND DISCUSSION

The parameters of overall molecular tumbling calculated by the approach outlined above are given in Table 3 with respect to the axis system defined in Fig. 2. The correlation times $\tau_x$, $\tau_y$, $\tau_z$, $\tau_+$, and $\tau_-$ calculated from the experimental data according to Eq. [A4] (in the Appendix) are given in Table 4.

To assess the quality of the fit the experimental dipolar longitudinal relaxation times are compared to those back-calculated from the minimization results for the overall and internal motions in Table 5.

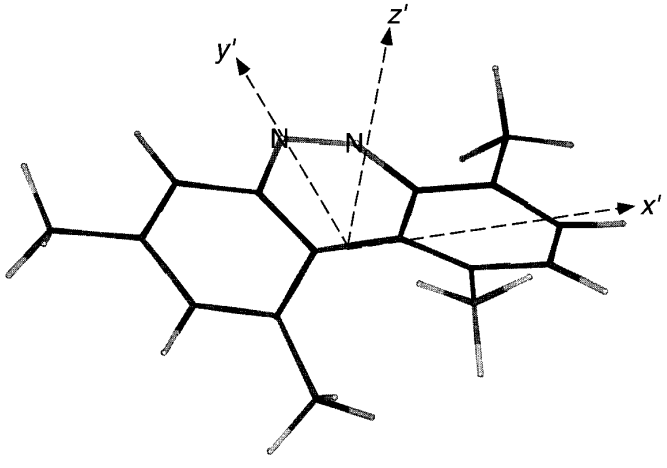


**FIG. 2.** Optimized 3D structure of **II** and its inertial axes obtained with the cff91 force field of InsightII. The Cartesian coordinates are given in Table 2.

In the theory of diffusion on which our calculations are based it is assumed that the duration of a jump is short compared to the time between two jumps. A simple test of the validity of this assumption is the $\chi$ test [see (*10, 32, 33*)]. The value of $\chi$ is defined as

$$\chi_i = \frac{5}{18R_i}\sqrt{\frac{kT}{I_i}}, \qquad [3]$$

where the subscript $i$ refers to Cartesian axes. The arbitrary, but generally accepted, classification is that with $\chi > 5$ the assumption of diffusion control is justified, which is the case for the experiments carried out.

The internal rotational diffusion constants $W_i$ calculated

**TABLE 3**

**Overall Rotational Tumbling Rates $R$ for II Derived from the Experimental Data in Table 1 with Respect to the Inertial Axis System and the Geometry Given in Fig. 2 and Table 2[a]**

| Axis | $R$ (rad$^2$ s$^{-1}$) | $\Delta R$ | $I$ (kg m$^2$) | $\chi$ | $\Delta\chi$ |
|---|---|---|---|---|---|
| $x$ | $3.50 \times 10^9$ | $\pm 0.20 \times 10^9$ | $1.07 \times 10^{-44}$ | 46.0 | ±2.7 |
| $y$ | $1.89 \times 10^9$ | $\pm 0.10 \times 10^9$ | $2.45 \times 10^{-44}$ | 56.3 | ±3.0 |
| $z$ | $9.92 \times 10^9$ | $\pm 1.00 \times 10^9$ | $3.21 \times 10^{-44}$ | 9.4 | ±1.0 |

[a] The first column gives the calculated rotational diffusion constants $R_i$. The second column contains the error margin for $R_i$, which was estimated by repeating the minimization with relaxation parameters set to the limits of their respective error ranges. In the third column the calculated moments of inertia are given. The fourth and fifth columns list $\chi$ (defined in Eq. [3]) and its error margin arising from the propagation of errors in $R_i$ and $T$.

**TABLE 5**

**Comparison of Experimental Dipolar Longitudinal Relaxation Times with Those Back-Calculated on the Basis of the Minimization Results**

| C atom No. | $T_{1dd}^{calc}$ (s) | $T_{1dd}^{exp}$ (s) | ± (exp.) (s) |
|---|---|---|---|
| 2 | 1.39 | 1.35 | ±0.08 |
| 9 | 1.46 | 1.48 | ±0.08 |
| 8 | 1.26 | 1.15 | ±0.15 |
| 4 | 1.52 | 1.5 | ±0.1 |
| 1-$CH_3$ | 2.00 | 2.0 | ±0.1 |
| 10-$CH_3$ | 1.89 | 1.89 | ±0.09 |
| 3-$CH_3$ | 4.98 | 5.3 | ±0.3 |
| 7-$CH_3$ | 4.49 | 4.5 | ±0.25 |

are summarized in Table 6. The correlation times for internal rotations are (*14*) $\tau_i = (3W_i)^{-1}$.

A $\chi$ test is also applicable to internal rotations, with $\chi_W$ defined as (*17*)

$$\chi_W = \frac{3}{2\pi} * \frac{1}{W} * \sqrt{\frac{kT}{I_i}}\,. \qquad [4]$$

As can be seen from Table 6 methyl group 3 appears to be rotating under inertial rather than diffusion control. Therefore the calculated jump rate determined for this methyl group must be regarded with caution. The two sterically ''free'' methyl groups exhibit significantly different jump rates. The slowdown of methyl group 7 can be attributed to the effect of *ortho* substitution. The data on methyl jump rates in *ortho*- and *meta*-xylene at 263 K (*17*) also corroborate this: The methyl jump rate in *m*-xylene is given as $4.65 \times 10^{12}$ s$^{-1}$, whereas in *o*-xylene it equals $2.72 \times 10^{11}$ s$^{-1}$, a factor of 17 lower. The jump rates of the sterically free methyl groups 3 and 7 in compound **II** differ only by a factor of 7, probably due to the lower Van der Waals volume of the nitrogen atom (7 Å$^3$) compared to that of a methyl group (22.7 Å$^3$) (*34*). Methyl group 3 is surrounded only by hydrogen atoms at the *ortho* position, whose Van der Waals volumes are even smaller.

The sterically hindered methyl groups 1 and 10 are rotating more than 40 times slower around their $C_3$ axes than the ''unhindered'' methyl groups 3 and 7. The difference in jump rates between $CH_3$-1 and $CH_3$-10 is insignificant at the experimental error level and therefore cannot be used to draw conclusions on the existence or absence of correlated (cogwheel type) rotation. Activation parameters can be calculated from the jump rates using (*7, 17*)

$$V_0 = RT * \ln\left(\frac{3}{2W_i}\sqrt{\frac{kT}{I_{Me}}}\right), \qquad [5]$$

where $I_{Me}$ is the moment of inertia of a methyl group. $V_0$ characterizes the hindrance of the intramolecular rotation (*7, 17*) relative to a sterically ''free'' methyl group. It corresponds neither to the activation energy nor to the potential barrier of methyl rotation. The jump rate of $CH_3$-10 corresponds to an activation parameter $V_0 = 12.2$ kJ mol$^{-1}$, which is to our knowledge among the highest barriers determined so far for methyl group rotation [a compilation of methyl group rotational barriers can be found in Ref. (*17*)]. Comparison of activation parameters from different sources must be done with caution, because the numerical values depend strongly on the underlying motional models (*6, 17*). A study performed with the same motional model as is used here (*9*) reports 10.1 kJ mol$^{-1}$ for $CH_3$-11 and 8.8 kJ mol$^{-1}$ for $CH_3$-10 of 1,2,3,4-tetrahydro-5,6-dimethyl-1,4-methanonaphthalene (**III**). The molecular environment of $CH_3$-11 is similar to that of the two methyl groups in *o*-xylene. Apparently, the intermethyl repulsion in our model compound (**II**) is compensated mostly by the distortion of the aromatic skeleton rather than leading to mutual penetration of the space occupied by methyl groups, which should result in cogwheel interactions. Another important fact that must be borne in mind is that many earlier studies have been performed on neat liquids for sensitivity reasons, while dilute solutions have been used here to avoid intermolecular effects.

In order to be able to compare the mutual penetration of

**TABLE 4**

**Overall Correlation Times $\tau_x$, $\tau_y$, $\tau_z$, $\tau_+$, and $\tau_-$ Calculated from the Experimental Data in Table 3**

| | |
|---|---|
| $\tau_x$ | $3.87 \times 10^{-11}$ |
| $\tau_y$ | $4.77 \times 10^{-11}$ |
| $\tau_z$ | $2.22 \times 10^{-11}$ |
| $\tau_+$ | $2.21 \times 10^{-11}$ |
| $\tau_-$ | $6.29 \times 10^{-11}$ |

**TABLE 6**
**Jump Rates of Internal Methyl Group Rotation Calculated from Experimental Data[a]**

| $CH_3$ | $W$ ($s^{-1}$) | $\Delta W$ ($s^{-1}$) | $\chi_W$ | $\Delta\chi_W$ | $\tau_i$ | $\Delta\tau_i$ | $V_0$ (kJ $mol^{-1}$) | $\Delta V_0$ (kJ $mol^{-1}$) |
|---|---|---|---|---|---|---|---|---|
| 1 | $4.8 \times 10^{10}$ | $\pm 0.2 \times 10^{10}$ | 83 | ±3 | $6.9 \times 10^{-12}$ | $\pm 0.3 \times 10^{-12}$ | 12.0 | ±0.1 |
| 3 | $2.0 \times 10^{12}$ | $\pm 0.5 \times 10^{12}$ | 2.0 | ±0.5 | $1.7 \times 10^{-13}$ | $\pm 0.4 \times 10^{-13}$ | 3.9 | ±0.6 |
| 7 | $2.9 \times 10^{11}$ | $\pm 0.2 \times 10^{11}$ | 13.6 | ±0.1 | $1.1 \times 10^{-12}$ | $\pm 0.1 \times 10^{-12}$ | 8.1 | ±0.3 |
| 10 | $4.3 \times 10^{10}$ | $\pm 0.15 \times 10^{10}$ | 92 | ±3 | $7.7 \times 10^{-12}$ | $\pm 0.3 \times 10^{-12}$ | 12.2 | ±0.1 |

[a] The error margins are estimated in the same way as for the overall rotational diffusion constants. $\chi_W$ values are given, based on $I_{Me} = 5.2 \times 10^{-47}$ kg $m^2$ (*9*). The error margin of $\chi_W$ takes into account the errors arising from the uncertainties of $W$ and $T$. $\tau_i$ values are the correlation times of the internal rotations and $V_0$ is the activation parameter for the internal rotation.

methyl groups between different molecules from their three-dimensional structures, we need a new measure. Existing measures of methyl sterical hindrance such as the apparent overlap (*2*) refer to a static, planar canonical structure. Therefore they convey little information pertaining to the fraction of sterical hindrance which is relieved by skeletal distortion and thus has no direct significance for the methyl rotation barriers or mutual penetration. The ''methyl group interaction volume'' $V_{MM}$ we use is defined by the intersection of two methyl volumes. Each methyl volume encloses the Van der Waals volumes of the constituent atoms as averaged by rotation around the methyl $C_3$ axis (see Fig. 3). Since it is calculated from a three-dimensional structure it is a better gauge for the fraction of sterical hindrance affecting methyl rotation. X-ray crystallographic structures, if available, are superior to structures from molecular mechanics calculations, since most molecular mechanics parameter sets

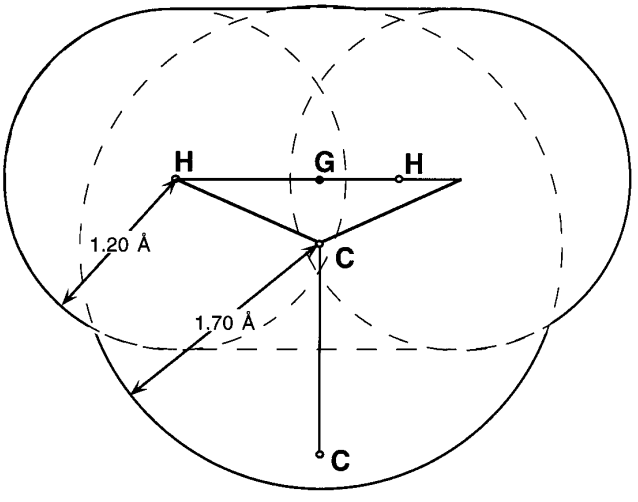


**FIG. 3.** Cross section of the methyl group volume used for the calculation of $V_{MM}$, which is composed from a methyl C-centered sphere with radius 1.7 Å [Van der Waals radius of carbon (*34*)] and an ''oblate'' centered at the center of gravity (G) of the three methyl protons with a height of 2.4 Å, which is enclosing all spheres with radius 1.2 Å [Van der Waals radius of hydrogen (*34*)] at any possible methyl H position.

are not optimized for this kind of interaction. In contrast to using a spherical approximation of the volume occupied by a single methyl group, $V_{MM}$ also takes care of the relative orientations of methyl axes. It turned out that in order to account for differences in the fitting of the methyl hydrogen atom positions into X-ray electron density maps, idealized methyl geometries must be used to calculate $V_{MM}$. The positions of methyl protons are calculated from the positions of the methyl carbon and of the atom it is attached to. A compilation of methyl group interaction volumes of compounds used in related studies is given in Table 7 and related to jump rates of methyl groups in similar environments. From this table it becomes clear that compounds analogous to 4,5-dimethylphenanthrene like **II** have an extremely high intermethyl penetration and are therefore suited best to the investigation of intermethyl interactions.

To estimate the effect of deviations of the rotational diffusion principal axis system from the inertial frame on the jump rates of methyl groups, the minimization was repeated for several relative orientations of these frames. The results show that the orientation of the diffusion tensor bears little influence on the jump rates of the sterically hindered methyl groups. Within ±10° for each of the three Euler angles and their combinations no deviations larger than $0.4 \times 10^{10}$ $s^{-1}$ for the jump rates of the sterically hindered methyl groups 1 and 10 were found. Even for the sterically free methyl group 7 deviations are not too severe (up to $0.6 \times 10^{11}$ $s^{-1}$), though outside the experimental error margin. The values for methyl group 3 contain large systematic errors due to the violations of other assumptions as mentioned above and should therefore be ignored in this context. The considerable changes in the overall tumbling are a numerical consequence of changing the reference system and do not indicate physically different rotational diffusion behavior.

## CONCLUSION

We have for the first time determined jump rates of sterically closely interacting methyl groups in an ''open six-ring'' juxtaposition as found in compounds of the 4,5-di-

**TABLE 7**

**Methyl Group Interaction Volumes[a] for Several Compounds of Interest, Representing the Structural Types Indicated in the Last Column, Where Available Jump Rates Extrapolated to 260 K Are Also Given**

| Compound (X ray) | Ref | $V_{MM}$ (Å$^3$) | $W$ (s$^{-1}$) | Compound (jump rates) | Ref. | Substructure type |
|---|---|---|---|---|---|---|
| 4a-Allyl-3,5,7,8,10-pentamethyl-4a,5-dihydroisoalloxazine | (*37*) | 1.8 | $2.27 \times 10^{11}$ | *o*-Xylene | (*17*) | *o*-Xylene |
| 1,8-Dimethylnaphthalene | (*38*) | 1.8 | | | | |
| (+)-3,3′-*p*-Chlorobenzylidene-bis(bornan-2-one) | (*39*) | 2.7 | $6.2 \times 10^{10}$<br>$9.9 \times 10^{10}$ | Camphor | (*7*) | Geminal |
| 9,10-Dihydro-4,5-dimethylphenanthrene | (*2*) | 2.9 | | | | |
| 4,5-Dimethylphenanthrene | (*1*) | 3.6 | $4.3 \times 10^{10}$<br>$4.8 \times 10^{10}$ | **II** | This paper | ''Open six-ring'' |
| 3,4,5,6-Tetramethylphenanthrene | (*1*) | 3.2 | | | | |

[a] The volume of a single methyl group determined according to Fig. 3 is 33 Å$^3$.

methylphenanthrene type. The methyl interaction volumes we introduced as a gauge for mutual penetration of methyl groups appear to be in qualitative agreement with the observed jump rates (with the cautionary restriction that for none of the compounds were both a crystallographic structure and jump rates available, and thus structures of similar compounds have been compared). By extrapolating from the slowdown in methyl rotational diffusion occurring between *m*- and *o*-xylene (Table 7) one would expect that in the case of the sterically hindered methyl groups in compound **II** a more pronounced slowdown should occur. Surprisingly the jump rates determined actually lie only slightly below those of geminal methyl groups in terpenes (*7*).

It might be speculated that the relief of steric strain by distortions of the molecular skeleton is not the only reason a further slowdown of methyl rotational diffusion in compounds of this type is prevented. With increasing methyl interaction volume cogwheel-like synchronized jumps can be taken into consideration. Although the probability of such concerted motions is lower than for a normal single methyl 120° jump, the fraction of synchronized methyl jumps would experience a lower barrier, thus increasing the observed jump rate. The fraction of concerted jumps will increase at lower temperatures. Our current experimental data do not provide direct evidence for such a mechanism and attempts to find evidence for cross-correlation effects in proton NMR spectra so far have been unsuccessful. Tang and co-workers (*35*, *36*) have investigated this problem by multiple-quantum $^1$H NMR in an oriented phase. They used 1,8-dimethylnaphthalene as a model compound, which has a smaller methyl group interaction volume than **II** (Table 7). We believe that compounds of the type studied here are better suited to future investigations of correlated methyl rotational diffusion, for which the results presented here will also serve as a starting point.

## APPENDIX

The dipolar spectral density of a spin pair undergoing totally anisotropic overall rotational tumbling and rotational diffusion around a single internal axis was given by Bluhm (*14*) as

$$
\begin{aligned}
J_h(\omega) = K_h \Bigg[ & \frac{A_0 12R(\omega^2 + 36L^2) + B_0 12(\omega^2 - 36L^2)}{\left(\frac{1}{\tau_+^2} + \omega^2\right)\left(\frac{1}{\tau_-^2} + \omega^2\right)} \\
& + \frac{A_T 2\left(\frac{1}{\tau_T} + 6R\right)\left(\omega^2 + \frac{1}{\tau_{+T}\tau_{-T}}\right) + B_T 12\left(\omega^2 - \frac{1}{\tau_{+T}\tau_{-T}}\right)}{\left(\frac{1}{\tau_{+T}^2} + \omega^2\right)\left(\frac{1}{\tau_{-T}^2} + \omega^2\right)} \\
& + \frac{A_S 2\left(\frac{1}{\tau_S} + 6R\right)\left(\omega^2 + \frac{1}{\tau_{+S}\tau_{-S}}\right) + B_S 12\left(\omega^2 - \frac{1}{\tau_{+S}\tau_{-S}}\right)}{\left(\frac{1}{\tau_{+S}^2} + \omega^2\right)\left(\frac{1}{\tau_{-S}^2} + \omega^2\right)} \\
& + \frac{C_{100}\tau_1}{1 + \omega^2\tau_1^2} + \frac{C_{101T}\tau_{1T}}{1 + \omega^2\tau_{1T}^2} + \frac{C_{101S}\tau_{1S}}{1 + \omega^2\tau_{1S}^2} \\
& + \frac{C_{200}\tau_2}{1 + \omega^2\tau_2^2} + \frac{C_{201T}\tau_{2T}}{1 + \omega^2\tau_{2T}^2} + \frac{C_{201S}\tau_{2S}}{1 + \omega^2\tau_{2S}^2} \\
& + \frac{C_{300}\tau_3}{1 + \omega^2\tau_3^2} + \frac{C_{301T}\tau_{3T}}{1 + \omega^2\tau_{3T}^2} + \frac{C_{301S}\tau_{3S}}{1 + \omega^2\tau_{3S}^2} \Bigg] \quad , \qquad [A1]
\end{aligned}
$$

where all $A_i$, $B_i$, and $C_i$ are coefficients depending on motional and geometrical parameters. Their definitions are also given in Ref. (*14*). The correlation times occurring in Eq. [A.1] are defined as follows:

$$\frac{1}{\tau_{+T}} = \frac{1}{\tau_+} + \frac{1}{\tau_T}, \quad \frac{1}{\tau_{1S}} = \frac{1}{\tau_1} + \frac{1}{\tau_S}$$
$$\frac{1}{\tau_{+S}} = \frac{1}{\tau_+} + \frac{1}{\tau_S}, \quad \frac{1}{\tau_{2T}} = \frac{1}{\tau_2} + \frac{1}{\tau_T}$$
$$\frac{1}{\tau_{-T}} = \frac{1}{\tau_-} + \frac{1}{\tau_T}, \quad \frac{1}{\tau_{2S}} = \frac{1}{\tau_2} + \frac{1}{\tau_S}$$
$$\frac{1}{\tau_{-S}} = \frac{1}{\tau_-} + \frac{1}{\tau_S}, \quad \frac{1}{\tau_{3T}} = \frac{1}{\tau_3} + \frac{1}{\tau_T}$$
$$\frac{1}{\tau_{1T}} = \frac{1}{\tau_1} + \frac{1}{\tau_T}, \quad \frac{1}{\tau_{3S}} = \frac{1}{\tau_3} + \frac{1}{\tau_S}. \qquad [A2]$$

$R$ and $L$ are defined by

$$R = \frac{R_1 + R_2 + R_3}{3}$$
$$L^2 = \frac{R_1R_2 + R_1R_3 + R_2R_3}{3}. \qquad [A3]$$

$\tau_1$, $\tau_2$, $\tau_3$, $\tau_+$, and $\tau_-$ are defined by

$$\tau_1^{-1} = 4R_1 + R_2 + R_3, \quad \tau_3^{-1} = R_1 + R_2 + 4R_3$$
$$\tau_2^{-1} = R_1 + 4R_2 + R_3, \quad \tau_\pm^{-1} = 6(R \pm \sqrt{R^2 - L^2}). \qquad [A4]$$

They belong to the overall tumbling, whereas the correlation times for the internal rotation, $\tau_T$ and $\tau_S$, are defined by

$$\frac{1}{\tau_T} = 2W_1 + W_2, \quad \frac{1}{\tau_S} = 2W + W_2, \qquad [A5]$$

where $W$, $W_1$, and $W_2$ are the jump rates as defined by Tsutsumi (*40*). The constants $K_h$ are defined by

$$K_0 = \tfrac{4}{5}$$
$$K_1 = \tfrac{2}{15}$$
$$K_2 = \tfrac{8}{15}. \qquad [A6]$$

Woessner's formula for the spectral density of the dipolar interaction between two spins in a rigid fragment with totally anisotropic reorientation is (*11*)

$$J_h(\omega) = K_h\left(\frac{C_+\tau_+}{1 + \omega^2\tau_+^2} + \frac{C_-\tau_-}{1 + \omega^2\tau_-^2} + \frac{C_1\tau_1}{1 + \omega^2\tau_1^2} + \frac{C_2\tau_2}{1 + \omega^2\tau_2^2} + \frac{C_3\tau_3}{1 + \omega^2\tau_3^2}\right) \qquad [A7]$$

with all $\tau_i$ as already given in Eq. [A.4] and

$$C_+ = d - e, \qquad C_2 = 6l'^2n'^2$$
$$C_- = d + e, \qquad C_3 = 6l'^2m'^2$$
$$C_1 = 6m'^2n'^2, \qquad [A8]$$

where

$$d = \frac{1}{2}(3(l'^4 + m'^4 + n'^4) - 1)$$
$$e = \frac{1}{6}(\delta_1(3l'^4 + 6m'^2n'^2 - 1) + \delta_2(3m'^4 + 6l'^2n'^2 - 1) + \delta_3(3n'^4 + 6l'^2m'^2 - 1))$$
$$\delta_i = \frac{R_i - R}{\sqrt{R^2 - L^2}} \qquad [A9]$$

and $l'$, $m'$, and $n'$ are the direction cosines of the internuclear vector in the rotational diffusion axis system of the molecule. $R$ and $L$ are defined in Eq. [A3].

## ACKNOWLEDGMENTS

This work was supported by the FWF (Austrian Science Foundation, Project P10571-CHE) and by the NFR (Norges forskningsråd, KAS scholarship for R.W.).

## REFERENCES

1. R. N. Armstrong, H. L. Ammon, and J. N. Darnow, *J. Am. Chem. Soc.* **109,** 2077 (1987).
2. R. Cosmo, T. W. Hambley, and S. Sternhell, *J. Org. Chem.* **52,** 3119 (1987).
3. H. V. Ansell and R. Taylor, *J. Org. Chem.* **44,** 4946 (1979).
4. K. H. Ladner, D. K. Dalling, and D. M. Grant, *J. Phys. Chem.* **80,** 1783 (1976).
5. K. F. Kuhlmann and D. M. Grant, *J. Chem. Phys.* **55,** 2998 (1971).
6. J. W. Blunt and J. B. Stothers, *J. Magn. Reson.* **27,** 515 (1977).
7. A. Ericsson, J. Kowalewski, T. Liljefors, and P. Stilbs, *J. Magn. Reson.* **38,** 9 (1980).
8. G. C. Levy, A. Kumar, and D. Wang, *J. Am. Chem. Soc.* **105,** 7536 (1983).
9. A. Dölle and T. Bluhm, *Mol. Phys.* **1986,** 721 (1986).
10. R. T. Boeré and R. G. Kidd, *Annu. Rep. NMR Spectrosc.* **13,** 319 (1982).

*11.* D. E. Woessner, *J. Chem. Phys.* **37,** 647 (1962).

*12.* D. E. Woessner, *J. Chem. Phys.* **36,** 1 (1962).

*13.* D. E. Woessner, *J. Chem. Phys.* **42,** 1855 (1965).

*14.* T. Bluhm, *Mol. Phys.* **47,** 475 (1982).

*15.* J. McEnerney, D. Neal, and P. Marunhic, Think Pascal V. 4.0, Symantec Corp., Cupertino (1988).

*16.* A. Dölle and T. Bluhm, *Prog. NMR Spectrosc.* **21,** 175 (1989).

*17.* T. Bluhm, *Mol. Phys.* **52,** 1335 (1984).

*18.* L. G. Werbelow and D. M. Grant, *Adv. Magn. Res.* **9,** 189 (1977).

*19.* L. G. Werbelow and D. M. Grant, *J. Chem. Phys.* **63,** 544 (1975).

*20.* W. Buchner, *J. Magn. Reson.* **12,** 82 (1973).

*21.* W. Buchner, *J. Magn. Reson.* **17,** 229 (1975).

*22.* L. G. Werbelow and D. M. Grant, *Can. J. Chem.* **55,** 1558 (1977).

*23.* N. Müller, *Monatsh. Chem.* **120,** 801 (1989).

*24.* N. Müller, G. Bodenhausen, and R. R. Ernst, *J. Magn. Reson.* **75,** 297 (1987).

*25.* N. Müller and G. Bodenhausen, *J. Chem. Phys.* **98,** 6062 (1993).

*26.* C. Coupry, M.-T. Chenon, and L. G. Werbelow, *J. Chem. Phys.* **101,** 899 (1994).

*27.* K. Raner, MacCurveFit V. 1.2, Kevin Raner Software, Mt. Waverley (1995).

*28.* J. Schleucher, M. Sattler, and C. Griesinger, *Angew. Chem.* **114,** 1518 (1993).

*29.* A. G. Palmer III, J. Cavanagh, P. E. Wright, and M. Rance, *J. Magn. Reson.* **93,** 151 (1991).

*30.* L. E. Kay, P. Keifer, and T. Saarinen, *J. Am. Chem. Soc.* **114,** 10663 (1992).

*31.* BIOSYM/MolecularSimulations, InsightII V. 2.9.7&95.0/3.00, BIOSYM/MSI, San Diego (1995).

*32.* K. T. Gillen and J. H. Noggle, *J. Chem. Phys.* **53,** 801 (1970).

*33.* D. Wallach and W. T. Huntress, *J. Chem. Phys.* **50,** 1219 (1969).

*34.* A. Bondi, *J. Phys. Chem.* **68,** 441 (1964).

*35.* J. Tang, W. Jinfeng, and A. Pines, *Sci. Sin., Ser. A* **30,** 157 (1987).

*36.* J. Tang and A. Pines, *J. Chem. Phys.* **72,** 3290 (1980).

*37.* R. Norrestam, *Acta Crystallogr. Sect. B* **28,** 1713 (1972).

*38.* D. Bright, I. E. Maxwell, and J. deBoer, *J. Chem. Soc. Perkin Trans. 2* 2101 (1973).

*39.* R. Roques, J. Sotiropuolos, J. P. Declerq, and G. Germain, *Acta Crystallogr. Sect. B* **37,** 1938 (1981).

*40.* A. Tsutsumi, *Mol. Phys.* **37,** 111 (1979).